

Modulation of Chondrocyte Phenotype for Tissue Engineering by Designing the Biologic–Polymer Carrier Interface

Tahir A. Mahmood,^{*,†,‡,§} Sylvie Miot,^{||} Oliver Frank,^{||} Ivan Martin,^{||} Jens Riesle,[†] Robert Langer,[‡] and Clemens A. van Blitterswijk[†]

Institute of Biomedical Technology, University of Twente, Prof. Bronkhorstlaan 10, 3723 MB Bilthoven, The Netherlands, Department of Chemical Engineering, Massachusetts Institute of Technology, 45 Carleton Street E25-342, Cambridge, Massachusetts 02139, and Division of Research, University of Basel Hospital, Hebelstrasse 20, Basel 4031, Switzerland

Received May 18, 2006

Therapeutic strategies based on cell and tissue engineering can be advanced by developing material substrates that effectively interrogate the biological compartment, with or without the complimentary local release of growth factors. Poly(ether ester) segmented copolymers were engineered as model material systems to elucidate the interfacial molecular events that govern the function of adhered cells. Surface chemistry was modulated by varying poly(ethylene glycol) (PEG) length and mole fraction with poly(butylene terephthalate) (PBT), leading to differential competitive protein adsorption of fibronectin and vitronectin from serum and consequently to different cell attachment modes. Adhesion within the hydrogel-like milieu of longer surface PEG was mediated via binding to the CD44 transmembrane receptor, rather than the RGD-integrin mechanism, whereas greater substrate-bound fibronectin resulted in cell adhesion via integrins. These adhesion modalities differentially impacted morphological cell phenotype (spread or spheroid) and the subsequent expression of mRNA transcripts (collagen types II, I) characteristic of phenotypically differentiated or dedifferentiated chondrocytes, respectively. These results demonstrate that materials can be designed to directly elicit the membrane bound receptor apparatus desired for downstream cellular response, without requiring exogenous biological growth factors to enable differentiated potential.

Introduction

Clinical bioengineering therapies, such as cell and tissue engineering, can involve the use of material substrates as delivery systems by which to transplant cells to diseased, damaged, or resected tissue. Once placed into the patient, hybrid material–biologic constructs allow the transplanted cells, or induce cells at the periimplant site, to produce tissue extracellular matrix (ECM) or endogenous growth factors required for tissue regeneration or repair.¹ Strategies employed to achieve the desired cellular response include the use of exogenous growth factors to enable differentiated potential,² as well as incorporation of peptide ligands or growth factors within the delivery substrate to induce bioactive functionality.³ However, little is understood regarding the mechanistic interfacial events that have the potential to regulate cell function without the use of exogenous bioactive growth factors or coatings.

For the development of such composite material–cellular technologies, it is necessary to understand the interaction between the material surface and the cellular/biological compartment, from protein adsorption to cell adhesion and downstream intracellular events. Cell–material interaction was first studied to understand the cultivation of anchorage-dependent mammalian cells on culture substrates^{4–6} and more recently for

cell delivery applications.^{7–9} Several substrate properties have been proposed as potential regulators of cell function, including surface wettability, flexibility, and roughness.¹⁰ In serum containing culture conditions, however, cells would be expected to “sense” the biochemical environment including proteins adsorbed at the surface, and not simply the native material chemistry. It has been suggested that a combination of substrate parameters collectively influence cell function by modulating the adsorption of proteins, with the resulting proteinaceous milieu at the surface impacting cell function.^{11,12}

A major challenge in current chondrocyte cell therapy arises from interactions between the cells and their delivery substrates. Chondrocyte attachment and spreading on surfaces is known to lead to “dedifferentiation” to a more fibroblast-like cell type, i.e., loss of Hyaline cartilage ECM protein synthesis (type II collagen and aggrecan), and the upregulation of type I collagen synthesis.^{13–17} In addition, it has been shown that the presence of fibronectin (Fn) can induce chondrocyte dedifferentiation in monolayer culture.^{18,19} Vitronectin (Vn) has also been shown to be involved in chondrocyte adhesion to some synthetic polymer substrates.²⁰

Segmented poly(ether ester) copolymers of poly(ethylene glycol)–terephthalate (PEGT) and poly(butylene terephthalate) (PBT) (PEGT:PBT) were synthesized as model substrates for studying material-directed cell function and cell transplantation, due to the flexibility in design afforded by the constituent polymers. This polymer system is also currently under evaluation as a substrate for tissue engineering applications. Copolymer properties are determined by the two components—the PEG segments contain mobile hydrophilic chains to provide a hydrogel-like local environment, whereas PBT provide hydro-

* To whom correspondence should be addressed. Phone 1.805.447.1000, E-mail: tmahmood@amgen.com.

† University of Twente.

‡ Massachusetts Institute of Technology.

§ Present address: Department of Pharmaceuticals, Amgen, One Amgen Center Drive, M/S 8-2-D, Thousand Oaks, CA 91320.

|| University of Basel Hospital.

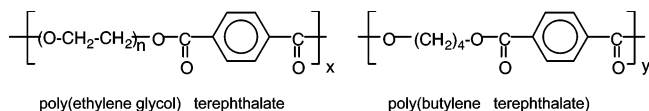


Figure 1. Chemical structure of segmented poly(ether ester) [PEGT:PBT] copolymers, formed by polycondensation polymerization of hydrophilic PEG-containing segments and hydrophobic PBT segments.

Table 1. List of Compositions of the Model PEGT:PBT Segmented Copolymer System, per the Nomenclature Used in This Study

| polym compsn, per applied nomenclature | PEG molecular mass | PEGT:PBT mass ratio |
|--|--------------------|---------------------|
| 4000-PEG 55:45 | 4000 | 55:45 |
| 1000-PEG 70:30 | 1000 | 70:30 |
| 1000-PEG 55:45 | 1000 | 55:45 |
| 1000-PEG 40:60 | 1000 | 40:60 |
| 300-PEG 70:30 | 300 | 70:30 |
| 300-PEG 55:45 | 300 | 55:45 |
| 300-PEG 30:70 | 300 | 30:70 |
| TCPS (tissue culture polystyrene) | n/a | n/a |

phobic, protein-binding domains and rigidity to the hybrid system²¹ (Figure 1). During synthesis, the molecular mass of PEG and the weight ratio of the PEGT:PBT components can be tailored to endow polymer substrates with specific surface and mechanical properties, as dictated by individual cell delivery applications.

The objective of this study was to elucidate the effects of varying model poly(ether ester) copolymer substrate parameters on the differential regulation of cell phenotype and to identify interactions between materials, proteins, and cells at the interfacial level that contribute to material-based cell regulation without the use of biological growth factors or coatings.

Methods

Polymer Preparation. (a) Synthesis. PEGT:PBT segmented copolymers were prepared by two-step condensation in the presence of titanium tetrabutoxide (Merck; Darmstadt, Germany) as catalyst (0.1 wt %).²¹ Vitamin E (Sigma; Uithoorn, The Netherlands) was included as an antioxidant for the polymers. Compositions were varied by changing the PEG molecular mass and the PEG to dimethyl terephthalate/1,4-butanediol (Merck) ratio.

(b) Polymer Nomenclature. The different formulations of this copolymer system are indicated as follows: *a*-PEG *b*:*c*, where *a* is the molecular mass of PEG (g/mol), *b* is the mass percentage of PEGT, and *c* is the mass percentage of the PBT component. For example, the copolymer 300-PEG 55:45 has PEG molecular mass of 300 g/mol and a PEGT:PBT ratio of 55:45. Tissue culture polystyrene (TCPS) was included as a control surface. A list of polymer compositions engineered for this study per the nomenclature used is provided in Table 1.

Substrate Preparation. Solutions of 20% (w/v) polymer in either chloroform (Sigma) or in a mixture of chloroform and 1,1,1,3,3,3-hexafluoro-2-propanol (Sigma) were cast into two-dimensional (2D) polymer substrate films (60–100 μm thick) on glass. The polymer substrates were placed in ethanol (12 h) to remove residual solvent, vacuum-dried under N₂ (48 h), γ-sterilized, and immersed in serum-containing culture medium (12 h) prior to cell seeding. The wettabilities of individual polymer compositions have been tested and reported previously.^{22,23}

Tissue Harvesting and Cell Isolation. Non-osteoarthritic articular cartilage was harvested from the femoral heads of female patients undergoing hip replacement surgery, under institutional standards of informed consent at the University Hospital of Basel. A representative set of complete data from one 65-year old female patient was selected. Primary chondrocytes were isolated by type II collagenase (Worthington Biochemical, Lakewood, NJ) digestion for 20 h, rinsed in phosphate buffered saline (PBS) containing CaCl₂ and MgCl₂ at pH 7.4 (Invitrogen; Breda, The Netherlands) with 15% fetal bovine serum (FBS) (Invitrogen), and transferred to a well-defined culture medium (Dulbecco's Modified Eagle Medium (DMEM) containing 4.5 g/L glucose and supplemented with 10% FBS, 1 mM sodium pyruvate (Invitrogen), 50 μg/mL penicillin, 50 μg/mL streptomycin, 0.4 mM L-proline, 0.1 mM nonessential amino acids, and 10 mM Hepes buffer (Sigma)).

Once isolated, cells were seeded at a density of 10 000 cells/cm² on each polymer. Attached cells were quantitated as described below at 1, 13, and 19 days after seeding, assessed morphologically, and analyzed for phenotypic mRNA transcript expression at day 19. All samples were evaluated in duplicate. The limited sample sizes were due to the difficulty in obtaining sufficient grossly non-osteoarthritic human cartilage from one biopsy, which was necessary for a consistent baseline cellular phenotype.

Real Time Quantitative Polymerase Chain Reaction (RT-PCR). Samples were frozen in Trizol reagent (Sigma) at –80 °C after harvesting at day 19. RNA were extracted using Trizol. cDNA were generated by using Stratascript reverse transcriptase (Stratagene, Amsterdam, The Netherlands) in the presence of dNTP according to the manufacturer's instructions. PCR reactions were performed and monitored using a ABI Prism 7700 sequence detection system (Perkin-Elmer Applied Biosystems). The PCR master mix was based on AmpliTaq Gold DNA polymerase (Perkin-Elmer Applied Biosystems). cDNA samples were analyzed in duplicates. Sequences of primers and probes for human collagen type I and II have been described previously.²⁴ After an initial denaturation step at 95 °C for 10 min, the cDNA products were amplified with 50 PCR cycles, consisting of a denaturation step at 95 °C for 15 s and an extension step at 60 °C for 1 min. Data analysis was carried out using the Sequence Detector V program (Perkin-Elmer Applied Biosystems). Since type II collagen is a typical marker of differentiated chondrocytes in Hyaline cartilage as opposed to type I collagen (expressed by dedifferentiated chondrocytes in fibrocartilage), the ratio of mRNA levels of collagen type II to I (CII/CI) was used as a useful "differentiation index" by which to compare chondrocyte differentiation.²⁴

Immunofluorescence Analysis of Receptors. At day 19 of culture, cells were fixed for 15 min with 4% paraformaldehyde (Sigma), rinsed with PBS (Invitrogen), and blocked for 30 min with serum-free protein block (DAKO, Glostrup, Denmark). Cells were further rinsed with PBS and incubated separately with each of the following monoclonal antibodies: anti-α5β1 PID6 (Covance, Princeton NJ), dilution 1:500; anti-αvβ3 VI-PL2 (Pharmingen, San Diego CA), dilution 1:100; anti-CD44/FITC BU52 (Ancell, Bayport MN), dilution 1:100. Cells were washed in PBS and further incubated for 30 min with appropriate secondary antibodies (Molecular Probes) except for the pre-conjugated anti-CD44. Cells were then washed 3 times with PBS prior to mounting with an antifading medium (Vectashield: Vector Labs, Burlingame, CA) and cover-slipping.

Although it is not yet possible to discriminate between occupied and unoccupied integrins visualized by immunofluo-

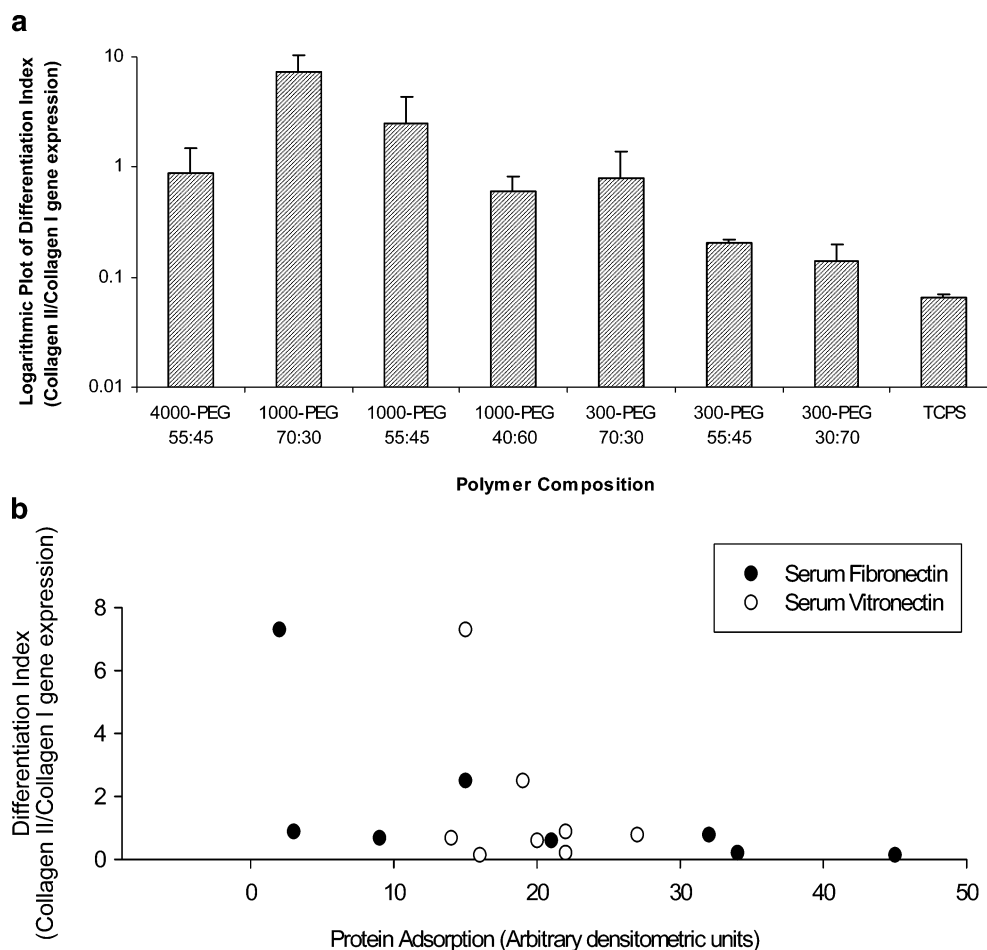


Figure 2. Chondrocyte CII/CI mRNA expression on substrates with varying PEG molecular mass and PEGT:PBT ratio (a, top), and CII/CI mRNA expression compared against Fn and Vn adsorption (b, bottom). The correlation between Fn adsorption and dedifferentiation was significant. In a, polymer compositions are arranged from left by PEG molecular mass of 4000, 1000, and 300 g/mol.

rescence microscopy, integrin occupancy does not preclude anti- $\alpha 5 \beta 1$ mAb binding to distinct epitopes on the integrin subunits. The secondary mAb used in these studies is known to inhibit the binding of $\alpha 5 \beta 1$ to a secondary synergy Pro-His-Ser-Arg-Asn (PHSRN) binding sequence in Fn, but does not block the recognition of the RGD motif,^{25,26} thereby leaving open the possibility that a population of such integrins may have bound to Fn in a manner that did not include the synergy sequence. Similarly, the BU52 anti-CD44 mAb binds to CD44 while allowing concomitant binding to the GAG-rich epitope.^{27,28} However, there is little information available regarding anti- $\alpha v \beta 3$ mAb peptide mapping.

Scanning Electron Microscopy (SEM). To examine cell morphology, samples harvested at day 19 were fixed in Karnovsky's fixative and dehydrated by a graded ethanol series and hydroxymethylsilazane (Sigma). Samples were sputter-coated (10 nm) with gold (Cressington Scientific, Watford, U.K.) and examined by SEM (Phillips ESEM, Eindhoven, The Netherlands).

Protein Adsorption and Desorption. Protein adsorption was studied by immersing 500 μ m diameter PEGT:PBT particles of eight different compositions overnight in FBS at 37 °C. The particles were then washed three times with PBS to remove passively attached proteins and boiled in Laemmli buffer (Bio-Rad, Veenendaal, The Netherlands) with 5% β -mercaptoethanol (Sigma; 15 min) to desorb proteins that had chemisorbed at the surface. Particles were centrifuged, and the supernatant (20 μ L) from each polymer composition was normalized to total protein desorbed (RC-DC protein assay: Bio-Rad), and were loaded

into lanes of SDS-polyacrylamide gels. To test whether all proteins had desorbed, the polymer particles were reboiled in Laemmli buffer and reevaluated for protein content, which was nondetectable.

Western Blotting. Samples were electrophoresed at 120 V. Decasted gels were soaked in blot buffer for 15 min and transferred to an Immobilon-P membrane (Millipore, Amsterdam, The Netherlands) by blotting for 1 h at 60 V, 120 mA. Blots were blocked by 30 min incubation in PBS/0.5% Tween X-100 (Sigma)/2% gelatin (CalBiochem, San Diego CA). This was followed by 4 h incubation at room temperature (RT) with either of the primary antibodies. The primary antibodies used were IST-3 anti-human Fn mAb (Sigma) and anti-bovine Vn pAb (Biotrend, Cologne, Germany). Blots were rinsed 3 \times 10 min in PBS/0.5% Tween X-100 followed by incubation for 1 h at RT in PBS/0.5% Tween X-100/2% gelatin plus the appropriate AP-conjugated secondary antibodies (Sigma), followed by rinsing 3 \times 10 min in PBS/0.5% Tween X-100. Detection was performed using a colorimetric AP conjugate substrate kit (Bio-Rad).

Semiquantitative Image Analysis. Stained blots were digitally scanned and relative quantities of Vn and Fn determined by automated histogram-based counting of dark versus white pixels, based on specified threshold values. The results are depicted on a scale of arbitrary densitometric units where the amount of dark pixels were normalized to the fixed overall band area.

Cell Quantitation. Quantitation of total DNA was performed by Cyquant cell proliferation assay kit (Molecular Probes,

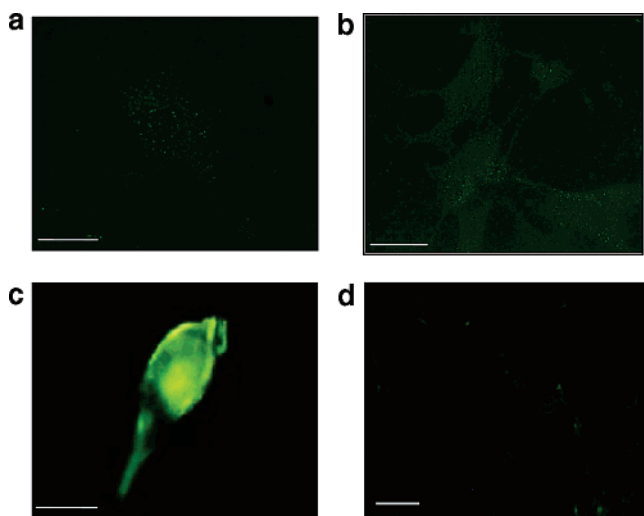


Figure 3. Immunofluorescence images of the Vn receptor $\alpha v \beta 3$ (a, top left), Fn receptor $\alpha 5 \beta 1$ (b, top right) expressed by chondrocytes cultivated on 300-PEG 55:45 substrates, as well as the proteoglycan receptor CD44 expressed by chondrocytes cultivated on 1000-PEG 70:30 (c, bottom left) and on 300-PEG 55:45 (d, bottom right) at day 19. Scale bars: (a) 20, (b) 40, (c) 10, and (d) 50 μm . The larger field of view in d demonstrated the negligible expression of CD44 by chondrocytes cultivated on 300-PEG 55:45.

Leiden, The Netherlands) using a spectrofluorometer (Perkin-Elmer, IL). Cell numbers were derived from DNA content by using results which show that there is 10 pg of DNA/(human chondrocyte).²⁹

Statistical Analysis. Analysis of significance (two-tailed distribution) was performed to study the correlation between polymer contact angle, cell attachment, CII/CI ratio, and Fn and Vn adsorption (SPSS, Chicago IL).

Results

The phenotype-modulating effects of the polymer materials are reported first, followed by an examination of the underlying mechanisms involved in the cellular and molecular response.

Analysis of mRNA Transcript Expression by Real Time PCR. Quantitative analyses of type II and type I collagen messenger RNA (mRNA) expression in cells cultivated for 19 days revealed the highest collagen II:collagen I (CII/CI) mRNA ratio for chondrocytes cultured on 1000-PEG 70:30 films (CII/CI = 7.3; Figure 2a). The lowest CII/CI mRNA ratios were found on the TCPS controls (CII/CI = 0.065). Cells on the 300-PEG 70:30 substrates demonstrated a marginally higher CII/CI mRNA ratio than those on 1000-PEG 40:60, whereas chondrocytes on the remaining 300 g/mol surfaces had lower CII/CI mRNA ratios than on any other PEGT:PBT substrate. Within the 1000 g/mol PEG group, only 1000-PEG 40:60 (CII/CI = 0.6) had a CII/CI mRNA ratio of less than 1 (Figure 2a).

Plots of CII/CI mRNA ratios versus either Fn or Vn revealed a significant inverse correlation with Fn adsorption (significant to the 0.05 level (two-tailed)), but no correlation with Vn (Figure 2b). However, chondrocyte CII/CI mRNA expression ratios plotted against surface contact angles indicated no direct correlation (data not presented).

Receptor Expression. Immunofluorescence microscopy at day 19 revealed the expression of the Vn-receptor $\alpha v \beta 3$ integrin and of the Fn-receptor $\alpha 5 \beta 1$ integrin at the focal adhesions of chondrocytes cultivated on PEGT:PBT substrates with 300 g/mol PEG (Figure 3a,b). The data presented here are from 300-PEG 55:45 substrates and are representative of the 300 g/mol

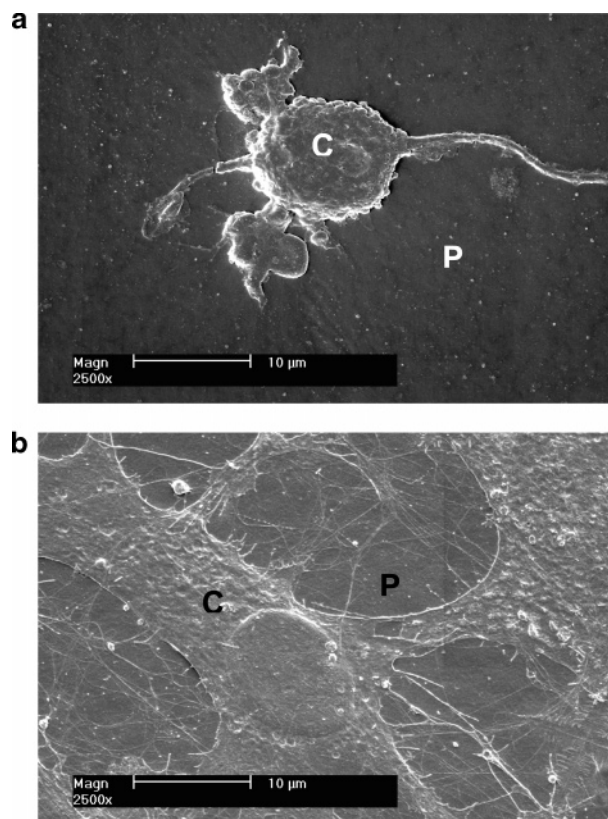


Figure 4. SEM images of a rounded chondrocyte on 1000-PEG 70:30 (a, top) and chondrocytes with spread morphologies on 300-PEG 30:70 (b, bottom), both at 19 days postseeding. Cells and polymer substrate are identified by the labels "C" and "P", respectively.

PEG polymers. No Fn- or Vn-integrin receptors were detected in cells cultured on 1000 g/mol polymers at any time point (data not presented).

Immunofluorescence imaging for CD44, a proteoglycan transmembrane receptor, revealed strikingly different results. At day 19, CD44 was seen to be expressed abundantly in chondrocytes cultivated on 1000 g/mol PEG substrates (Figure 3c), but its expression was negligible in cells cultured on substrates with 300 g/mol PEG (Figure 3d).

Chondrocyte Morphology. Chondrocytes cultured on 4000-PEG 55:45 polymer substrates and all 1000 g/mol PEG substrates were spheroid in shape (Figure 4a), although spreading increased with polymer PBT content (not shown).

Cell morphology was generally spread on 300 g/mol PEG materials. Figure 4b shows an example of the spread, fibroblastic morphology on the composition with the lowest PEGT content (30%). Chondrocytes that were adhered to the control TCPS exhibited spread and near-confluent morphologies (not shown).

Protein Adsorption. Semiquantitative gel analysis of Western blots of fibronectin and vitronectin adsorbed to polymers of different compositions revealed adsorption trends that depended on polymer composition (Figure 5a). On the 4000-PEG 55:45 composition, there was 7 times more Vn than Fn. Polymer compositions with 1000 g/mol PEG molecular mass generally demonstrated increasing amounts of both Fn and Vn as the percentage of PEGT was reduced from 70 to 40% (i.e. decreasing wettability). However, there was a pronounced increase in Fn across the same range of decreasing wettability, with the relative amount of Fn compared to Vn increasing from almost 1:8 to 1:1.

On 300 g/mol PEG substrates, lower Fn but higher Vn adsorption correlated with wettability, as measured by captive

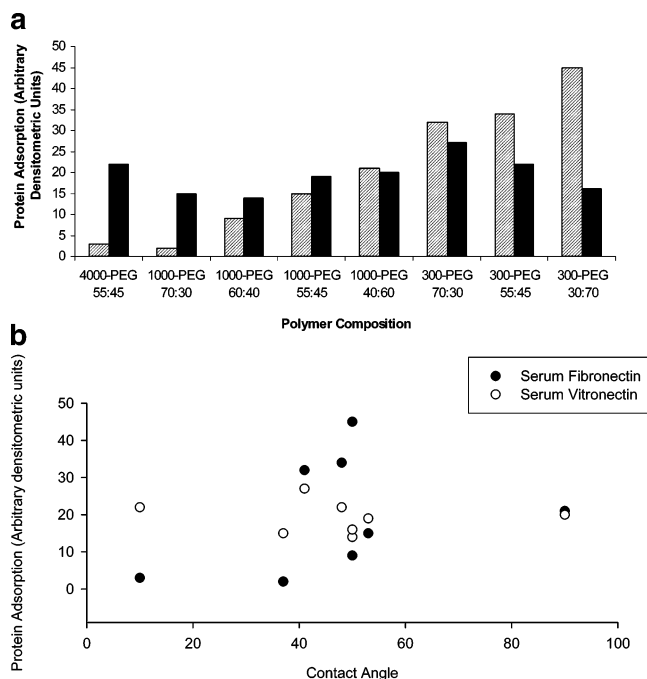


Figure 5. Relative adsorption of Vn and Fn on polymer substrates with varying PEG molecular mass and PEGT:PBT ratio (a, top). The bars correspond to Fn (clear) and Vn (solid). Polymers are arranged from left by PEG molecular mass of 4000, 1000, and 300 g/mol. Panel b relates the adsorption of Fn and Vn to substrate wettability.

bubble techniques on water-equilibrated polymer films. There was always greater adsorption of Fn on the 300 g/mol PEG polymers than either of the 1000 or 4000 g/mol PEG molecular weight ranges (Figure 5a).

When individual adhesive protein adsorption was plotted against substrate–water contact angle, Fn adsorption exhibited large variability in the 40–50° contact angle range (Figure 5b). Vn adsorption remained within a range, regardless of contact angle. There was no significant correlation between Vn or Fn adsorption and wettability.

Cell Attachment. Chondrocyte numbers were determined by quantitation of DNA in cell lysates 1 day after seeding (Figure 6a). The tissue culture polystyrene (TCPS) controls contained the most cells (17 400 cells/well). On PEGT:PBT polymer compositions, however, the highest cell attachment was seen on 300-PEG 30:70 (9200 cells/well). Polymers with the same length of PEG chains but with decreasing PEGT content exhibited higher cell numbers. This trend was seen at surfaces of each PEG molecular weight group. As the length of PEG molecules was shortened from 1000 to 300 g/mol while the PEGT:PBT ratio was held constant, cell attachment displayed an increase. Differences in cell number when PEG chain lengths were shortened from 4000 to 1000 g/mol were less pronounced. Although low at the lowest (10°) and highest (90°) contact angles, chondrocyte attachment increased on some substrates with contact angles between 40 and 54° (Figure 6b). However, cell attachment remained comparatively low on other substrates within the same general range of wettability, suggesting that wettability was not the sole parameter influencing chondrocyte attachment.

When chondrocyte attachment was examined as a function of protein adsorption, it was seen that the amount of Fn adsorbed directly correlated with cell attachment (correlation was significant at the 0.01 level (two-tailed); Figure 6c). However, no correlation could be made for cell attachment and Vn adsorption (Figure 6c).

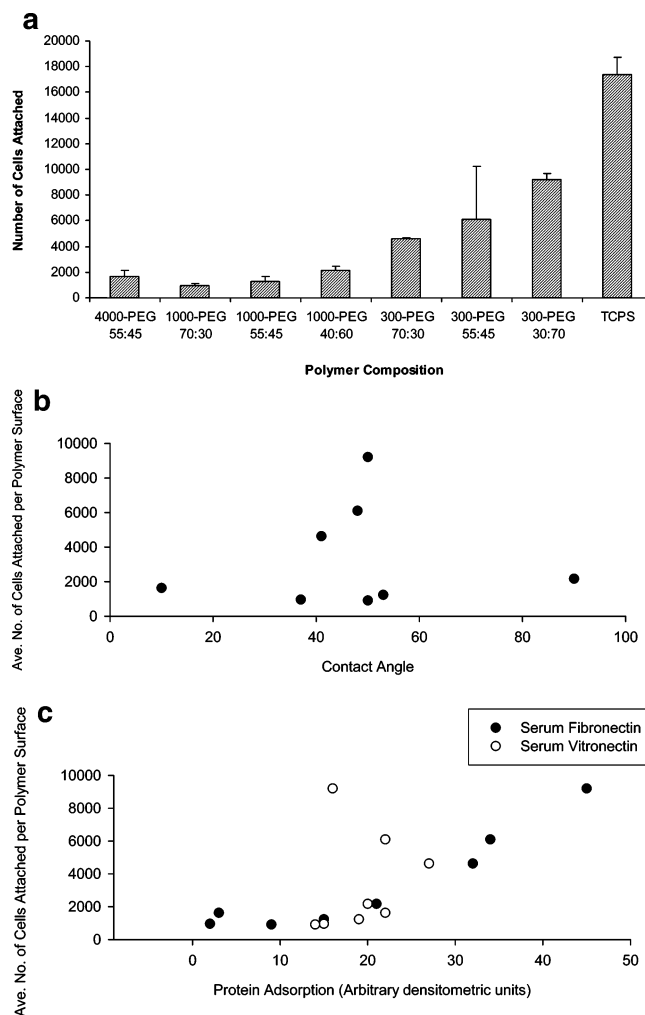


Figure 6. Average number of cells at day 1 attached to substrates with varying PEG molecular mass and PEGT:PBT ratio (a, top). Polymers are arranged from left by PEG molecular mass of 4000, 1000, and 300 g/mol. Substrate wettability versus cell number is plotted in b (middle). The relationship between cell number at day 1 and protein adsorption is demonstrated in c (bottom), where the correlation between cell attachment and Fn adsorption was significant.

Discussion

There has recently been considerable interest in the development of “smart materials” that are able to regulate the behavior of adhered or encapsulated cells by releasing bioactive molecules into the local environment or through extracellular protein/peptide mimetics built into the delivery substrates.^{30,31} However, the ability of materials to modulate downstream gene response without exogenous growth factors, coatings, or complex ligand incorporation has the potential to greatly facilitate the development of tissue engineering and cellular therapies. As an illustration of this concept, a class of biphasic calcium phosphate ceramic induced *de novo* bone formation at non-osseous sites *in vivo* without requiring the delivery of cells or biologic compounds,³² suggesting that the surface chemistry of the ceramic allowed the selective adsorption of morphogenetic proteins that trigger osteogenesis. It was also demonstrated using polymer libraries that substrate chemistry can influence the developmental lineages of embryonic stem cells.³³ Our data presented here with chondrocytes cultivated on PEGT:PBT substrates compliment these results, demonstrating that certain materials have an intrinsic potential to induce highly specific cell behavior, including modulation of phenotype (Figures 2–4).

Our objective for this study was to shed light on the interfacial events that integrate the materials, proteins, cell surface receptors, and subsequent downstream gene expression by cells adhered to polymeric delivery substrates. Protein adsorption was shown to correlate with chondrocyte differentiation index and attachment (Figures 2b and 6c). Interestingly, examination of data as a function of contact angle revealed an independence of protein adsorption and chondrocyte attachment on substrate wettability (Figures 5 and 6). These analyses suggest that differential adhesion protein adsorption to materials, and not simply surface wettability, plays a significant role in regulating cell function. It should be noted, however, that since contact angles provide wettabilities that are integrated across the entire analyzed surface area, the actual situation is complex and is likely to be at least partially governed by the angstrom/nanoscale phase separated structure of the underlying PEGT:PBT surface, as described earlier for this class of polymers.³⁴

The pro-chondrogenic potential of specific compositions of poly(ether ester) copolymers may be explained by examining substrate–protein and protein–receptor interactions. PEG molecules in water are in a liquidlike state, with rapid movement and a large excluded volume, with high PEG content surfaces providing the greatest steric interference.³⁵ This is also applicable to the PEGT:PBT substrates synthesized and studied herein and was examined using PEG length and weight ratio. Changes in substrate composition and wettability have been shown to influence Fn conformation,³⁶ with conformational interplay between competitively adsorbed Fn and albumin at the material–protein interface enhancing FN activity.³⁷ The amount of surface PEG in other polymers has been shown to inversely correlate with Fn coating and affects its conformation.³⁸ The effects of protein folding have not been examined in this study, however, and is an area that needs further study with respect to the biomaterial interface. Both Vn and Fn can exist in either folded or extended conformations,^{39,40} binding to cells primarily via integrin binding to Arg-Gly-Asp (RGD) sequence domains,^{41,42} as well as by glycosaminoglycan (GAG)-binding motifs in the vicinity of the carboxyl terminus that bind to transmembrane proteoglycans.^{43–47} Normal differentiated chondrocytes express and bind to their hyaluronic acid-rich extracellular matrix via CD44, a proteoglycan transmembrane receptor that can also bind to the GAG-binding domains of the adsorbed proteins.⁴⁸ Therefore, we postulate that the differentiated chondrogenic phenotype observed on high-density PEG polymers was due to CD44–protein interaction via GAG-binding domains.

Interestingly, it has been previously reported that Vn adsorption was not inhibited by increasing PEG concentration at a surface, regardless of substrate wettability,⁴⁹ and that Vn adsorbed equally well to untreated PS as to surface-modified TCPS.⁵⁰ Both studies compliment our data that suggest that substrate wettability alone does not strongly influence Vn adsorption. Whereas native Vn does not have strong affinity for GAG, this affinity is greatly increased upon adsorption to surfaces due to the unfolding of the protein and subsequent exposure of GAG-binding domains.⁵¹ Since up to 20% of Vn in serum is already in the extended GAG-binding conformation,⁵¹ the likelihood of GAG-binding domains to be exposed to the chondrocyte plasma membrane is significant and would be in addition to any binding domain exposure by adsorption to the hydrophobic PBT domains of the polymer substrate.

Chondrocytes that exhibited higher chondrogenic gene expression (per the differentiation index) also maintained a spheroid morphology (Figures 3 and 4), whereas Fn adsorption

resulted in chondrocyte dedifferentiation by the formation of focal adhesion plaques containing the $\alpha 5 \beta 1$ integrin receptor (Figure 3). The relationship between cell shape and differentiation has been widely described,^{13,14,52} and we have previously shown that causing a change in cell shape by inhibiting RhoA activation enabled the reversion of the chondrogenic phenotype from a dedifferentiated state.⁵³ It was also recently reported that causing mesenchymal stem cells to conform to either a spread or spheroid shape differentially induced cell differentiation toward the osteogenic and adipogenic lineages, respectively, due to shape-driven influences in signaling pathways.⁵⁴ Chondrocytes from healthy human articular cartilage are known to express $\alpha 5 \beta 1$ integrin, whereas $\alpha v \beta 3$ is only weakly expressed.⁵⁵ However, in vitro monolayer culture on TCPS markedly increased surface expression of these integrins⁵⁶ and resulted in chondrocyte dedifferentiation. Since spheroid chondrocytes in vitro also show greater incorporation of $^{35}\text{SO}_4$ into GAG than spread chondrocytes,⁵⁷ the adsorption of Fn on substrates may also play a role in cell spreading, in addition to adhesion, and is a phenomenon not found in healthy cartilage in vivo.

In conclusion, this study suggests a strong role of material modification in creating biomimetic and cellular effects that, until now, were principally expected from biological moieties such as growth factors. This was illustrated by modulation of the chondrogenic phenotype through differential induction of cell-surface receptors that coincided with different quantities of substrate-bound Fn or Vn. These events influence cell shape and downstream gene expression and can be engineered by changing polymer composition to provide the molecular cues required for individual therapeutic applications.

Acknowledgment. We are grateful to Drs. M. Humphries and J. Bezemer for helpful discussions regarding this manuscript.

References and Notes

- (1) Langer, R.; Vacanti, J. Tissue engineering. *Science* **1993**, *260*, 920–926.
- (2) Tabata, Y. Tissue regeneration based on growth factor release. *Tissue Eng* **2003**, *9* (Suppl. 1), S5–15.
- (3) Chen, R. R.; Mooney, D. J. Polymeric growth factor delivery strategies for tissue engineering. *Pharm. Res.* **2003**, *20*, 1103–1112.
- (4) Stoker, M.; O'Neill, C.; Berryman, S.; Waxman, V. Anchorage and growth regulation in normal and virus-transformed cells. *Int. J. Cancer* **1968**, *3*, 638.
- (5) Maroudas, N. G. Sulphonated polystyrene as an optimal substratum for the adhesion and spreading of mesenchymal cells in monovalent and divalent saline solutions. *J. Cell Physiol.* **1977**, *90*, 511.
- (6) Curtis, A.; Forrester, J.; McInnes, C.; Lawrie, F. Adhesion of cells to polystyrene surfaces. *J. Cell Biol.* **1983**, *97*, 1500–1506.
- (7) Cima, L. et al. Tissue engineering by cell transplantation using degradable polymer substrates. *J. Biomech. Eng.* **1991**, *113*, 143–151.
- (8) Woodfield, T. B.; Bezemer, J. M.; Pieper, J. S.; van Blitterswijk, C. A.; Riesle, J. Scaffolds for tissue engineering of cartilage. *Crit. Rev. Eukaryotic Gene Expression* **2002**, *12*, 209–236.
- (9) Hunziker, E. B. Articular cartilage repair: Basic science and clinical progress. A review of the current status and prospects. *Osteoarthritis Cartilage* **2002**, *10*, 432–463.
- (10) Saltzman, W. M. In *Principles of Tissue Engineering*, 2nd ed.; Lanza, R. P., Langer, R., Vacanti, J., Eds.; Academic Press: San Diego, 2000; pp 221–235.
- (11) Horbett, T.; Schway, M. Correlations between mouse 3T3 cell spreading and serum fibronectin adsorption on glass and hydroxyethylmethacrylate–ethylmethacrylate copolymers. *J. Biomed. Mater. Res.* **1988**, *22*, 763–793.
- (12) Lee, M. H.; Ducheyne, P.; Lynch, L.; Boettiger, D.; Composto, R. J. Effect of biomaterial surface properties on fibronectin- $\alpha 5 \beta 1$ integrin interaction and cellular attachment. *Biomaterials* **2006**, *27*, 1907–1916.

- (13) Loty, S.; Forest, N.; Boulekbache, H.; Sautier, J. M. Cytochalasin D induces changes in cell shape and promotes in vitro chondrogenesis: A morphological study. *Biol. Cell* **1995**, *83*, 149–161.
- (14) Martin, I.; Vunjak-Novakovic, G.; Yang, J.; Langer, R.; Freed, L. E. Mammalian chondrocytes expanded in the presence of fibroblast growth factor 2 maintain the ability to differentiate and regenerate three-dimensional cartilaginous tissue. *Exp. Cell Res.* **1999**, *253*, 681–688.
- (15) Martin, I. et al. Enhanced cartilage tissue engineering by sequential exposure of chondrocytes to FGF-2 during 2D expansion and BMP-2 during 3D cultivation. *J. Cell Biochem.* **2001**, *83*, 121–128.
- (16) Benya, P. D.; Shaffer, J. D. Dedifferentiated chondrocytes reexpress the differentiated collagen phenotype when cultured in agarose gels. *Cell* **1982**, *30*, 215–224.
- (17) Wang, L.; et al. Flow cytometric analysis of the human articular chondrocyte phenotype in vitro. *Osteoarthritis Cartilage* **2001**, *9*, 73–84.
- (18) Pennypacker, J. P.; Hassell, J. R.; Yamada, K. M.; Pratt, R. M. The influence of an adhesive cell surface protein on chondrogenic expression in vitro. *Exp. Cell Res.* **1979**, *121*, 411–415.
- (19) West, C. M.; et al. Fibronectin alters the phenotypic properties of cultured chick embryo chondroblasts. *Cell* **1979**, *17*, 491–501.
- (20) Wyre, R. M.; Downes, S. The role of protein adsorption on chondrocyte adhesion to a heterocyclic methacrylate polymer system. *Biomaterials* **2002**, *23*, 357–364.
- (21) Deschamps, A. A.; Grijpma, D. W.; Feijen, J. Poly(ethylene oxide)/poly(butylene terephthalate) segmented block copolymers: The effect of copolymer composition on physical properties and degradation behavior. *Polymer* **2001**, *42*, 9335–9345.
- (22) Papadaki, M.; et al. The different behaviors of skeletal muscle cells and chondrocytes on PEGT/PBT block copolymers are related to the surface properties of the substrate. *J. Biomed. Mater. Res.* **2001**, *54*, 47–58.
- (23) Deschamps, A. A.; et al. Design of segmented poly(ether ester) materials and structures for the tissue engineering of bone. *J. Controlled Release* **2002**, *78*, 175–186.
- (24) Martin, I.; et al. Quantitative analysis of gene expression in human articular cartilage from normal and osteoarthritic joints. *Osteoarthritis Cartilage* **2001**, *9*, 112–118.
- (25) Mould, A. P.; et al. Defining the topology of integrin $\alpha 5 \beta 1$ -fibronectin interactions using inhibitory anti- $\alpha 5$ and anti- $\beta 1$ monoclonal antibodies. *J. Biol. Chem.* **1997**, *272*, 17283–17292.
- (26) Burrows, L.; Clark, K.; Mould, A. P.; Humphries, M. J. Fine mapping of inhibitory anti- $\alpha 5$ monoclonal antibody epitopes that differentially affect integrin-ligand binding. *Biochem. J.* **1999**, *344*, 527–533.
- (27) Okamoto, I.; et al. Regulated CD44 cleavage under the control of protein kinase C, calcium influx, and the Rho family of small G proteins. *J. Biol. Chem.* **1999**, *274*, 25525–25534.
- (28) Anstee, D.; et al. New monoclonal antibodies in CD44 and CD58: Their use to quantify CD44 and CD58 on normal human erythrocytes and to compare the distribution of CD44 and CD58 in human tissues. *Immunology* **1991**, *74*, 197–205.
- (29) Jakob, M.; et al. Enzymatic digestion of adult human articular cartilage yields a small fraction of the total available cells. *Connect. Tissue Res.* **2003**, *44*, 173–180.
- (30) Anderson, D. G.; Burdick, J. A.; Langer, R. Materials science. Smart biomaterials. *Science* **2004**, *305*, 1923–1924.
- (31) Lutolf, M. P.; Hubbell, J. A. Synthetic biomaterials as instructive extracellular microenvironments for morphogenesis in tissue engineering. *Nat. Biotechnol.* **2005**, *23*, 47–55.
- (32) Yuan, H. P.; et al. A comparison of the osteoinductive potential of two calcium phosphate ceramics implanted intramuscularly in goats. *J. Mater. Sci.: Mater. Med.* **2002**, *13*, 1271–1275.
- (33) Anderson, D. G.; Levenberg, S.; Langer, R. Nanoliter-scale synthesis of arrayed biomaterials and application to human embryonic stem cells. *Nat. Biotechnol.* **2004**, *22*, 863–866.
- (34) Dechamps, A. A.; Grijpma, D. W.; Feijen, J. Poly(ethylene oxide)/poly(butylene terephthalate) segmented block copolymers: The effect of copolymer composition on physical properties and degradation behavior. *Polymer* **2001**, *42*, 9335–9345.
- (35) Lee, J. H.; Kopecek, J.; Andrade, J. D. Protein-resistant surfaces prepared by PEO-containing block copolymer surfactants. *J. Biomed. Mater. Res.* **1989**, *23*, 351–368.
- (36) Altankov, G.; et al. Modulating the biocompatibility of polymer surfaces with poly(ethylene glycol): Effect of fibronectin. *J. Biomed. Mater. Res.* **2000**, *52*, 219–230.
- (37) Grinnell, F. Fibronectin adsorption on material surfaces. *Ann. N. Y. Acad. Sci.* **1987**, *516*, 280–290.
- (38) Tziampazis, E.; Kohn, J.; Moghe, P. V. PEG-variant biomaterials as selectively adhesive protein templates: model surfaces for controlled cell adhesion and migration. *Biomaterials* **2000**, *21*, 511–520.
- (39) Erickson, H. P.; Carrell, N. A. Fibronectin in extended and compact conformations. Electron microscopy and sedimentation analysis. *J. Biol. Chem.* **1983**, *258*, 14539–14544.
- (40) Williams, E. C.; Janmey, P. A.; Ferry, J. D.; Mosher, D. F. Conformational states of fibronectin. Effects of pH, ionic strength, and collagen binding. *J. Biol. Chem.* **1982**, *257*, 14973–14978.
- (41) Ruoslahti, E.; Pierschbacher, M. D. Arg-Gly-Asp: A versatile cell recognition signal. *Cell* **1986**, *44*, 517–518.
- (42) Suzuki, S.; Oldberg, A.; Hayman, E. G.; Pierschbacher, M. D.; Ruoslahti, E. Complete amino acid sequence of human vitronectin deduced from cDNA. Similarity of cell attachment sites in vitronectin and fibronectin. *Embo J.* **1985**, *4*, 2519–2524.
- (43) Dalton, B. A.; McFarland, C. D.; Underwood, P. A.; Steele, J. G. Role of the heparin binding domain of fibronectin in attachment and spreading of human bone-derived cells. *J. Cell Sci.* **1995**, *108* (Pt 5), 2083–2092.
- (44) Liang, O. D.; Rosenblatt, S.; Chhatwal, G. S.; Preissner, K. T. Identification of novel heparin-binding domains of vitronectin. *FEBS Lett.* **1997**, *407*, 169–172.
- (45) Woods, A.; McCarthy, J. B.; Furcht, L. T.; Couchman, J. R. A synthetic peptide from the COOH-terminal heparin-binding domain of fibronectin promotes focal adhesion formation. *Mol. Biol. Cell* **1993**, *4*, 605–613.
- (46) Schwartz, I.; Seger, D.; Shaltiel, S. Vitronectin. *Int. J. Biochem. Cell Biol.* **1999**, *31*, 539–544.
- (47) Suzuki, S.; et al. Domain structure of vitronectin. Alignment of active sites. *J. Biol. Chem.* **1984**, *259*, 15307–15314.
- (48) Knudson, W.; Loeser, R. F. CD44 and integrin matrix receptors participate in cartilage homeostasis. *Cell. Mol. Life Sci.* **2002**, *59*, 36–44.
- (49) Fabrizio-Homan, D. J.; Cooper, S. L. Competitive adsorption of vitronectin with albumin, fibrinogen, and fibronectin on polymeric biomaterials. *J. Biomed. Mater. Res.* **1991**, *25*, 953–971.
- (50) Pitt, W. G.; Fabrizio-Homan, D. J.; Mosher, D. F.; Cooper, S. L. Vitronectin adsorption onto polystyrene and oxidized polystyrene. *J. Colloid Interface Sci.* **1989**, *129*, 231–239.
- (51) Preissner, K. T. Structure and biological role of vitronectin. *Annu. Rev. Cell Biol.* **1991**, *7*, 275–310.
- (52) Loty, C.; Forest, N.; Boulekbache, H.; Kokubo, T.; Sautier, J. M. Behavior of fetal rat chondrocytes cultured on a bioactive glass-ceramic. *J. Biomed. Mater. Res.* **1997**, *37*, 137–149.
- (53) Mahmood, T. A.; de Jong, R.; Riesle, J.; Langer, R.; van Blitterswijk, C. A. Adhesion-mediated signal transduction in human articular chondrocytes: The influence of biomaterial chemistry and tenascin-C. *Exp. Cell Res.* **2004**, *301*, 179–188.
- (54) McBeath, R.; Pirone, D. M.; Nelson, C. M.; Bhadriraju, K.; Chen, C. S. Cell shape, cytoskeletal tension, and RhoA regulate stem cell lineage commitment. *Dev. Cell* **2004**, *6*, 483–495.
- (55) Loeser, R. F. Chondrocyte integrin expression and function. *Biorheology* **2000**, *37*, 109–116.
- (56) Loeser, R. F.; Carlson, C. S.; McGee, M. P. Expression of beta 1 integrins by cultured articular chondrocytes and in osteoarthritic cartilage. *Exp. Cell Res.* **1995**, *217*, 248–257.
- (57) Glowacki, J.; Trepman, E.; Folkman, J. Cell shape and phenotypic expression in chondrocytes. *Proc. Soc. Exp. Biol. Med.* **1983**, *172*, 93–98.

BM060489+